Life Sciences 232 (2019) 116669

Contents lists available at ScienceDirect

Life Sciences

journal homepage: www.elsevier.com/locate/lifescie

Hyaluronic acid promotes osteogenic differentiation of human amniotic mesenchymal stem cells *via* the TGF-β/Smad signalling pathway

Ling-Tao Zhang[a], Ru-Ming Liu[a], Yi Luo[a], Yu-Jie Zhao[b], Dai-Xiong Chen[a], Chang-Yin Yu[a,c,*], Jian-Hui Xiao[a,**]

[a] Zunyi Municipal Key Laboratory of Medicinal Biotechnology, Center for Translational Medicine, Affiliated Hospital of Zunyi Medical University, 149 Dalian Road, Zunyi 563003, PR China
[b] Department of Laboratory Medicine, Affiliated Hospital of Zunyi Medical University, 149 Dalian Road, Zunyi 563003, PR China
[c] Department of Neurology, Affiliated Hospital of Zunyi Medical University, 149 Dalian Road, Zunyi 563003, PR China

ARTICLE INFO

Keywords:
Hyaluronic acid
Human amniotic mesenchymal stem cells
Osteogenic differentiation
TGF-β/Smad signalling pathway

ABSTRACT

Aims: This study investigated the effects of hyaluronic acid (HA), a commonly used osteogenic medium referred to as DAG, and the combined administration of HA and DAG (CG) on the osteogenic differentiation of human amniotic mesenchymal stem cells (hAMSCs), and the underlying mechanism.

Main methods: The phenotype of hAMSCs was detected by flow cytometry and immunocytochemical staining. Alkaline phosphatase (ALP) and calcium deposition assays were employed for evaluating the osteogenic differentiation of hAMSCs. The expression of osteogenesis-related genes and proteins was determined by quantitative reverse transcription PCR (qRT-PCR) and Western blotting, respectively. Meanwhile, the molecular mechanism of osteogenic differentiation of hAMSCs was detected by PCR array and qRT-PCR.

Key findings: The results showed that treatment with CG could significantly stimulate hAMSC ALP activity and calcium deposition compared to treatment with DAG, while HA had little effect. The expression of osteogenesis-related molecules and stemness-related molecules was up-regulated at the mRNA and protein levels in all three groups, and this up-regulation was most significant in the CG group. In addition, treatment with CG significantly increased the gene expressions involved in regulation of the TGF-β/Smad signalling pathway compared to treatment with DAG. Furthermore, the pro-osteogenic differentiation effects as well as the up-regulated expression of genes observed in the CG treatment group were significantly inhibited when the cells were pre-treated with SB431542, an inhibitor of the TGF-β/Smad pathway.

Significance: These results suggest that HA in combination with DAG could significantly enhance the osteogenic differentiation of hAMSCs, potentially *via* the TGF-β/Smad signalling pathway.

1. Introduction

Bone defects caused by trauma, infection, bone tumour excision, and other reasons are a major clinical challenge. Surgical techniques including autogenous bone grafting and the Ilizarov distraction technique are commonly employed to repair bone defects [1]. However, the use of these methods is restricted by the lack of available bone for the first approach, and the long treatment time needed for the second approach [2]. Stem cell-based bone tissue engineering is a promising approach that offers an alternative treatment option for repairing bone defects. Human amniotic mesenchymal stem cells (hAMSCs), a major type of adult mesenchymal stem cells, have a high capacity for self-renewal and can differentiate into different cell types such as bone (osteoblasts), cartilage (chondrocytes), and fat (adipocytes) [3]. Upon in vivo transplantation, hAMSCs are able to secrete a wide range of bioactive molecules, such as cellular growth factors and immunosuppressive factors, and create a microenvironment that promotes tissue repair and regeneration. Furthermore, hAMSCs present no risk of immunogenicity or tumorigenicity in vivo [4,5]. In addition, hAMSCs are isolated from the amniotic membrane after delivery, and as such are not considered to be controversial in terms of medical ethics. Thus, hAMSCs are potential candidates for stem cell transplantation therapy of repairing bone defects, whose efficient and directional osteogenic differentiation in vitro is an important issue.

** Correspondence to: J. H. Xiao, Zunyi Municipal Key Laboratory of Medicinal Biotechnology, Center for Translational Medicine, Affiliated Hospital of Zunyi Medical University, 149 Dalian Road, Zunyi 563003, PR China.
* Corresponding author.
E-mail addresses: yuchangyin68@163.com (C.-Y. Yu), jhxiao@zmc.edu.cn, jianhuixiao@126.com (J.-H. Xiao).

https://doi.org/10.1016/j.lfs.2019.116669
Received 28 March 2019; Received in revised form 17 July 2019; Accepted 17 July 2019
Available online 18 July 2019
0024-3205/

Hyaluronic acid (HA) is a linear non-sulphated glycosaminoglycan composed of repeating disaccharide units of N-acetyl-*D*-glucosamine and *D*-glucuronic acid that is widely found in body fluid and tissues, such as connective, epithelial, and skin tissues. It is a major structural component of the extracellular matrix in mammalian tissues, and regulates diverse biological processes, including cell proliferation, differentiation, migration, and adhesion, *via* receptors such as CD44 [6]. HA plays multiple roles in skeletal biology, including facilitating migration and condensation of mesenchymal cells, forming joint cavities, and promoting long bone growth; it also participates in bone remodelling by controlling osteoclast, osteoblast, and osteocyte behaviour [7,8]. Thus, HA could be used to regulate osteoblastic differentiation. Some recent studies have reported that HA regulates osteoblastic differentiation in different tissue-specific cell types. Huang et al. reported that HA induced osteoblastic differentiation in rat calvarial-derived mesenchymal cells through a molecular weight (MW)-specific mode of action, *i.e.*, low MW HA (60 kDa) increased cell proliferation and osteocalcin mRNA expression without osteoblastic differentiation, while high MW HA (900 and 2300 kDa) increased all of the parameters tested and induced osteoblastic differentiation [9]. In contrast, Nakata's research group found that high MW HA (900–1200 kDa) inhibited bone morphogenetic protein (BMP)-induced osteoblastic differentiation by signalling through the CD44 receptor in mouse myoblast cells and mouse bone marrow cells [10]. Another group reported that high MW HA (2000 kDa) enhanced BMP-2-induced osteogenic differentiation in a human osteoblastic cell line MG63 cells by down-regulating the expression level of BMP-2 antagonists (noggin and follistatin) and the phosphorylation level of ERK protein [11]. Therefore, the osteogenic bioactivity of HA is debatable, and it is unclear whether low MW HA (< 900 kDa) facilitates osteoblastic differentiation. We hypothesized that the regulatory properties of HA depended not only on its MW but also on the cell type.

HA-based hydrogel scaffolds are one of the most promising materials for bone tissue repair, because they are biodegradable and non-immunogenic. The scaffolds are typically constructed using HA alone and/or in combination with other components to improve their osteogenic potential. For example, HA hydrogel has been used as a carrier to deliver recombinant human BMP-2 (rhBMP-2). Ossipov's research group constructed a modified HA hydrogel containing an engineered integrin-specific ligand that effectively enhanced the osteogenic potential of rhBMP-2 [12]. Totey's group found that the use of a tripolymer combining chitosan, collagen type 1, and HA was more effective at enhancing osteoblastic differentiation and calcium deposition in human bone marrow-derived mesenchymal stem cells than each of the three individual polymers alone [13].

Therefore, HA has shown excellent application potential in the field of bone defect repair, either is used as osteogenic differentiation regulator directly or scaffold material. However, the regulatory role and mechanism of different molecular weight HA on osteogenic differentiation of different stem cells remain largely unknown. The aim of this study was to investigate the effects of low MW HA with 300 kDa on osteoblastic differentiation in hAMSCs, and to determine the underlying mechanism by which HA promotes osteoblastic differentiation.

2. Materials and methods

2.1. Reagents

HA (300 kDa MW) was purchased from Seebio Biotech, Inc. (Shanghai, China). Low- or high-glucose Dulbecco's Modified Eagle Medium (LG/HG-DMEM), trypsin, GlutaMAX, non-essential amino acids (NEAAs), foetal bovine serum (FBS), and β-mercaptoethanol were purchased from GIBCO Industries, Inc. (Langleg, OK, USA). D-Hank's buffer, phosphate-buffered saline (PBS), and antibiotics (penicillin and streptomycin) were obtained from Sino American Biotechnology Co. (Shanghai, China). Dexamethasone (DXM), β-glycerol phosphate disodium, L-ascorbic acid, collagenase II, DNase I, and Alizarin red S (ARS) were all purchased from Sigma-Aldrich, Inc. (St. Louis, MO, USA).

2.2. Isolation and primary culture of hAMSCs

The study and use of the human amnion were approved by the Ethics Committee of Affiliated Hospital of Zunyi Medical University (Zunyi, China). Primary hAMSCs were isolated from the placentas of healthy donors who delivered full-term babies by Caesarean using a mechanical and two-step enzymatic digestion procedure [4]. The cells were inoculated into 25-cm^2 cell culture flasks (Corning, NY, USA) at a density of 5×10^5 cells/flask in mesenchymal stem cell growth media (MSCGM), which consisted of LG-DMEM with 10% (*v*/v) FBS, 1% (v/v) L-GlutaMAX, 1% (v/v) NEAA, 55 μmol/L β-mercaptoethanol, 10 ng/mL bFGF, and 1% (v/v) antibiotics, and was maintained at 37 °C in an incubator with an atmosphere consisting of 5% CO_2, 95% air, and 100% relative humidity. The cell growth medium was replaced every three days, and the cells were passaged at 70% to 80% confluence. Cells at passage 3 (P3) were used for this study. All of the experiments were performed at least three times.

2.3. Phenotypic identification of hAMSCs

The hAMSCs were identified by flow cytometry on the basis of cell surface markers. For the flow cytometric analysis, a fluorescein isothiocyanate (FITC)-conjugated mouse anti-human CD90 monoclonal antibody, an allophycocyanin (APC)-conjugated mouse anti-human CD73 monoclonal antibody, a PerCP-Cy5.5-conjugated mouse anti-human CD105 monoclonal antibody, and phycoerythrin (PE)-conjugated mouse anti-human monoclonal CD44, CD34, CD11b, CD19, CD45, and HLA-DR antibodies were obtained from BD Pharmingen (San Diego, CA, USA). Isotype control fluorescent-labelled mouse IgG monoclonal antibodies (IgG1 κ-FITC, IgG1 κ-APC, IgG1 κ-PerCP-Cy5.5, IgG1 κ-PE, IgG2a κ-PE, IgG2b κ-PE), also from BD Pharmingen, were used as the controls. P3 hAMSCs in the logarithmic growth phase were harvested and washed twice with Dulbecco's PBS (D-PBS) containing 1% (m/v) bovine serum albumin. Cell viability was determined using trypan blue exclusion staining, after which 200 μL of the cell suspension at a density of 1.5×10^6 cells/mL was added to each tube and 10 μL of the directly conjugated CD antibodies listed above was added to each sample. Next, the cell suspensions were gently mixed by oscillation and incubated at room temperature in the dark for 25 min. Then, 2 mL of D-PBS containing 0.1% (m/v) NaN_3 was added to each tube. The tubes were centrifuged at 400 RCF for 5 min and the supernatant was discarded. The resulting cell pellet was re-suspended with 200 μL of D-PBS containing 4% (m/v) paraformaldehyde per tube and was analysed using the BD FACSCalibur flow cytometry (FCM) system and CellQuest software (BD, NJ, USA).

The hAMSCs were also identified using immunocytochemical staining (ICC) for mesenchymal cell biomarkers. For the ICC staining of cell smears, coverslips were placed in an optical grade 6-well plate under sterile conditions, then P2 hAMSCs were inoculated at a density of 2×10^5 cells/well and maintained at 37 °C in mesenchymal stem cell growth media in a 5% CO_2 incubator. The cell smear was taken out and washed three times with D-PBS for 5 min per wash when the cells were in the logarithmic growth phase. The cells were then fixed with 4% (m/v) paraformaldehyde at room temperature for 30 min. After three 5 min washes with D-PBS, the cells were permeabilized with 0.3% (*v*/v) Triton X-100 for 15 min at room temperature. Following three more washes with D-PBS, the cells were blocked with 3% (v/v) H_2O_2 for 10 min and 10% (v/v) normal goat serum for 30 min at room temperature in the dark. Then, the coverslips were washed and incubated at 4 °C overnight with or without mouse anti-human vimentin or cytokeratin 19 primary antibodies (Sigma, MO, USA); D-PBS was used instead of the primary antibody as the negative control. Next, the

coverslips were washed three times with D-PBS to remove the primary antibody and incubated with an HRP-conjugated secondary antibody (GenTech, Shanghai, China) at 37 °C for 30 min. The coverslips were washed three times for 5 min each, and then stained with 3′-diaminobenzidine tetrahydrochloride (DAB) for 3–5 min at room temperature. After washing with distilled water, the cells were counterstained with haematoxylin (Solarbio, Beijing, China).

2.4. hAMSC osteogenic experiments

For the osteogenic differentiation experiments, P3 hAMSCs were seeded in 6-well plates (Corning, NY, USA) at 2×10^5 per well in MSCGM, as described above. When the cells reached 50% confluence, they were treated with a final concentration of 0.1, 0.2, 0.5, or 1.0 mg/mL HA. The ideal concentration of HA, which was determined to be 0.5 mg/mL, was used for all of the subsequent experiments. The four treatment groups investigated in this study were: the negative control group (CON), the HA treatment group (HA), the positive drug control group (DAG), and the HG + DAG group (CG). For the CON group, hAMSCs were grown in MSCGM only. The HA group was supplemented with 0.5 mg/mL HA, the DAG group was supplemented with 100 nM DXM, 50 mg/L L-ascorbic acid, and 10 Mm β-glycerol phosphate disodium (a cocktail combination frequently referred to as DAG), and the CG group was supplemented with 0.5 mg/mL HA and DAG. For the long-term osteogenic differentiation experiments, the active ingredients listed above were added to each group when the medium was changed every three days.

2.5. Alkaline phosphatase (ALP) staining and enzymatic activity

hAMSCs cultured under the different osteogenic induction conditions for 7 days and 14 days were assayed for ALP staining and activity. ALP staining was performed using a 5-bromo-4-chloro-3-indolyl-phosphate (BCIP)/nitro-blue-tetrazolium (NBT) alkaline phosphatase colour development kit (Beyotime, Shanghai, China) following the standard procedures. ALP activity was quantified using an alkaline phosphatase assay kit (Beyotime, Shanghai, China) according to the manufacturer's protocol, and the absorbance at 405 nm was measured using a microplate reader (Multiskan™ GO, ThermoFisher, USA). The total protein content in the same sample was measured using a BCA protein assay kit (Beyotime, Shanghai, China). ALP activity relative to the control group was calculated after normalization to the total protein content. All of the experiments were performed in triplicate, and the results are representative of at least three independent experiments.

2.6. Mineralization assay and quantification

Mineralization (calcium deposition) of hAMSCs at 21 days was assayed and quantified by ARS staining. Prior to staining, the cell growth medium was removed from the hAMSCs, and the cells were washed three times with D-PBS for 5 min. The cells were then fixed with 4% paraformaldehyde at room temperature for 30 min. After another three washes, they were stained with 40 mM ARS for 5 min at room temperature. Subsequently, the cells were washed three times with D-PBS and images were taken. For quantitative determination of the degree of mineralization, the ARS stain bound by the differentiated osteoblasts was eluted at 37 °C for 30 min with 1 mL of 10% (m/v) cetylpyridinium chloride per well. Then, 100 μL/well of the eluted stain was transferred to a 96-well plate, and the absorbance of the eluted solution was measured at 562 nm using a Multiskan™ GO microplate spectrophotometer (Thermo Fisher Scientific, USA).

2.7. Quantitative reverse transcription PCR

The relative expression levels of osteogenic marker genes and stemness genes in cells grown under the different conditions were investigated at 7, 14, and 21 days after osteoinduction by real-time quantitative reverse transcription polymerase chain reaction (qRT-PCR), as described previously [4]. Briefly, total RNA was extracted from hAMSCs using the RNAiso Plus extraction kit (Takara Bio, Dalian, China) according to the manufacturer's instructions. The extracted RNA was treated with a DNase I solution to remove any contaminating DNA and further purified using a RNeasy® MinElute™ Cleanup Kit (Qiagen). The purity and concentration of the resulting RNA were measured using a NanoDrop™ 1000 spectrophotometer (Thermo Fisher Scientific, USA). cDNA was prepared from total RNA using the PrimeScript™ RT reagent kit (Perfect Real Time, Takara Bio, China), according to the manufacturer's instructions. A SYBR® Premix Ex Taq™ II kit (Perfect Real Time, Takara Bio, China) and a CFX96™ Real-Time PCR detection system (Bio-Rad, CA, USA) were used for the qRT-PCR analysis. The amplification protocol consisted of an initial denaturation and enzyme activation step at 95 °C for 30 s, followed by 40 cycles of 95 °C for 5 s and 60 °C for 30 s. β-actin was used as the internal control for mRNA expression levels. The primers used for qRT-PCR are shown in Table 1. Relative gene expression levels (the amount of target gene expression, normalized to

Table 1
Primer sequences of genes tested.

Gene	Sequence(5′ → 3′)	GI (accession)	Product length (bp)
RunX2	For: TCCACACCATTAGGGACCATC Rev: TGCTAATGCTTCGTGTTTCCA	NM_001024630.3 NM_001015051.3 NM_001278478.1	136
Osx	For: CCTCTGCGGGACTCAACAAC Rev: AGCCCATTAGTGCTTGTAAAGG	NM_001173467.2 NM_152860.1 NM_001300837.1	128
Ocn	For: CTCACACTCCTCGCCCTATT Rev: AACTCGTCACAGTCCGGATT	NM_199173.4	239
BSP	For: CCCCACCTTTTGGGAAAACCA Rev: TCCCCGTTCTCACTTTCATAGAT	NM_004967.3	109
Col1α1	For: GTGCGATGACGTGATCTGTGA Rev: CGGTGGTTTCTTGGTCGGT	NM_000088.3	119
ALP	For: GCGCAAGAGACACTGAAATATGC Rev: TGGTGGAGCTGACCCTTGAG	NM_000478.4 NM_001127501.2	140
4-Oct	For: AAGGATGTGGTCCGAGTGTG Rev: GAAGTGAGGGCTCCCATAGC	NM_002701.5 NM_203289.5 NM_001173531.2 NM_001285986.1 NM_001285987.1	180
Nanog	For: CCCCAGCCTTTACTCTTCCTA Rev: CCAGGTTGAATTGTTCCAGGTC	NM_024865.3	97
BMP5	For: ACGAAAGACGGGAAATACAAAGG Rev: CATAAAGAGAGGTGCAGAGGACG	NM_021073.2	107
GDF10	For: AGATCGTTCGTCCATCCAACC Rev: GGGAGTTCATCTTATCGGGAACA	NM_004962.3	108
TGF-β2	For: CCCCGGAGGTGATTTCCATC Rev: GGGCGGCATGTCTATTTTGTAAA	NM_003238.3 NM_001135599.2	140
SMAD2	For: CCGACACACCGAGATCCTAAC Rev: GAGGTGGCGTTTCTGGAATATAA	NM_005901.5 NM_001135937.2 NM_001003652.3	125
SMAD3	For: TGGACGCAGGTTCTCCAAAC Rev: CCGGCTCGCAGTAGGTAAC	NM005902.3 NM_001145102.1 NM_001145103.1 NM_001145104.1	90
SMAD4	For: CTCATGTGATCTATGCCCGTC Rev: AGGTGATACAACTCGTTCGTAGT	NM_005359.5	146
SMAD5	For: CCAGCAGTAAAGCGATTGTTGG Rev: GGGGTAAGCCTTTTCTGTGAG	NM_005903.6 NM_001001419.2 NM_001001420.2	220
β-Actin	For: TGGCACCCAGCACAATGAA Rev: CTAAGTCATAGTCCGCCTAGAAG	NM_001101.3	186

the internal control gene expression) were calculated using the $2^{-\Delta\Delta Ct}$ method.

2.8. Western blotting analysis

The relative expression level of each osteogenic protein under different conditions was measured at 7, 14, and 21 days after osteoinduction by Western blotting, as described previously [4]. In brief, the growth media were discarded, and the hAMSCs were washed 2–3 times with D-PBS. Total protein and/or nuclear proteins were isolated using total protein extraction and nuclear-cytosol extraction kits (Applygen, Beijing, China) following the manufacturer's protocols. The protein concentration was measured using a BCA protein assay kit (Beyotime, Shanghai, China) according to the manufacturer's instructions. Primary antibodies against RunX2, Osx, ALP, Col1α1, BSP, and β-actin (Abcam, Cambridge, UK) were diluted 1:1000 to 1:10000 and added to the membranes, which were then incubated at 4 °C overnight. After overnight incubation, any unbound primary antibodies were removed by washing the membranes three times for 5 min each with Tris-buffered saline. Subsequently, the membranes were incubated with horseradish peroxidase-conjugated goat anti-mouse or anti-rabbit IgG secondary antibodies (Abcam, Cambridge, UK) diluted 1:10,000 at room temperature for 1 to 2 h. The membranes were then rinsed three times for 5 min each with Tris-buffered saline. Finally, the membranes were visualized using an ECL kit (Beyotime, Shanghai, China). Band intensities were quantified using a ChemiDoc™ MP Imaging System (Bio-Rad, CA, USA) and Image J 1.46a software. The background was subtracted, and the signal of each target protein band was normalized to that of the loading control (β-actin) band.

2.9. Microarray and bioinformatics

Signalling pathway analysis was performed using the human osteogenesis RT^2 Profiler™ PCR array (PAHS-026Z, SABiosciences), which monitors 84 different genes associated with osteogenesis, according to the manufacturer's instructions. The 96-well PCR array also contains 12 internal control genes, including a panel of five housekeeping genes (ACTB, B2M, GAPDH, HPRT1, and RPLP0), a human genomic DNA contamination control, three reverse transcription controls, and three positive PCR controls. A 2× SuperArray PCR master mix (Cat. No. 330522) was used to amplify the cDNA from the hAMSC samples after osteoinduction, according to the manufacturer's instructions. The PCR program was as follows: an initial polymerase activation/denaturation step at 95 °C for 10 min, followed by 40 amplification cycles of 95 °C for 15 s and 60 °C for 1 min. The data were analysed using the SABiosciences web portal (http://pcrdataanalysis.sabiosciences.com). Gene expression levels were determined using the comparative Ct method. The values were normalized by subtracting the geometric mean of the Ct values for the housekeeping gene from the Ct value of each gene of interest. Housekeeping genes whose Ct values varied by > 2-fold among the conditions were excluded [14].

2.10. Statistical analysis

At least three independent replicates were performed for all of the experiments. Data are expressed as the mean ± standard deviation (SD). The statistical differences were analysed by one-way ANOVA and Student's *t*-test. *P*-values lower than 0.05 were considered to indicate statistical differences.

3. Results

3.1. hAMSCs phenotypes

As shown in Fig. 1, the hAMSCs used in the study expressed high levels of surface protein biomarkers, including CD90 (91.30 ± 5.31%), CD73 (91.22 ± 5.19%), CD105 (96.88 ± 3.28%), and CD44 (98.12 ± 3.49%), while the hematopoietic stem cell surface markers CD34, CD45, CD11b, CD19, and HLA-DR were either expressed at very low levels or not expressed at all. In addition, the hAMSCs showed strong, diffuse expression of vimentin, but did not express CK19. These results are consistent with the minimal criteria for defining human multipotent mesenchymal stromal cells as proposed by the Mesenchymal and Tissue Stem Cell Committee of the International Society for Cellular Therapy [15], and confirmed the mesenchymal origin of the cells.

3.2. Effect of HA on hAMSCs osteogenic differentiation

hAMSCs were induced for 7, 14, and 21 days under different osteoinduction conditions. Cell morphology and density were observed using an inverted microscope; the images are shown in Fig. 2A. hAMSCs in the DAG and CG treatment groups showed morphological changes at 7 days: the cells transitioned from the typical long-spindle morphology to short-spindle, triangle, or polygonal shapes with clear boundaries between the cells. However, hAMSCs treated with HA alone exhibited very little change in cell shape. After 14 days of treatment, hAMSCs in both the DAG and CG groups displayed a paving stone-like pattern. Then, 21 days post-osteoinduction, overlapping cell growth was observed, in addition to the formation of some light-tight cell nodules. By this time point, most of the long-spindle-shaped hAMSCs in the CON and HA groups also exhibited irregular shapes.

The differentiation of mesenchymal stem cells (MSCs) into osteoblasts is a crucial step in bone formation. ALP, an ectoenzyme secreted by mature osteoblasts, is an early phenotypic marker for osteogenic differentiation of stem cells. ALP activity is typically present on the seventh day after *in vitro* osteoinduction, and ALP staining is visible after 14 days of osteogenic induction [16]. However, both ALP activity and staining were apparent after 7 days of osteogenic induction by DAG and CG in the present study, as shown in Fig. 2B and D. There was no difference between the DAG and CG groups. A substantial increase in ALP expression was observed 14 days post-osteoinduction, and this expression was significantly higher in the CG treatment group than in the DAG treatment group, which suggests that HA has a marked synergistic effect in combination with DAG (a positive stimulator). However, the HA group did not exhibit ALP activity, and the ALP staining results were similar to those from the negative control group (CON), as shown in Fig. 2B and D.

Osteogenic differentiation of MSCs results in mineralization or the formation of osteoblast nodules, which is a marker for osteogenic differentiation. As such, on day 21 of the osteoinduction experiments, the formation of mineralized nodules in hAMSCs was assessed by Alizarin red S (ARS) staining, and the amount of mineralization was quantitated by eluting the ARS stain from the differentiated osteoblasts. As shown in Fig. 2C and E, treatment with HA alone only gave rise to negative or minimal ARS staining, similar to the negative control, indicating that the cells in the HA group did not display mineralization. The cells in the DAG and CG treatment groups exhibited characteristic osteoblast nodules. Furthermore, a significant increase in ARS staining was observed in the CG group compared with the DAG group, which was confirmed by quantitative analysis of ARS, as shown in Fig. 2E. Therefore, the results of the ALP activity and ARS staining assays demonstrated that HA in combination with DAG significantly promoted the osteogenic differentiation of hAMSCs, and that HA alone did not directly induce hAMSC osteogenesis.

3.3. Effect of HA on the expression of osteogenic differentiation-specific genes and proteins in hAMSCs

To determine the effect of HA on the molecular changes that occur during hAMSC osteogenic differentiation, we examined the relative expression levels of the osteogenesis-associated genes *RunX2*, *Osx*, *BSP*,

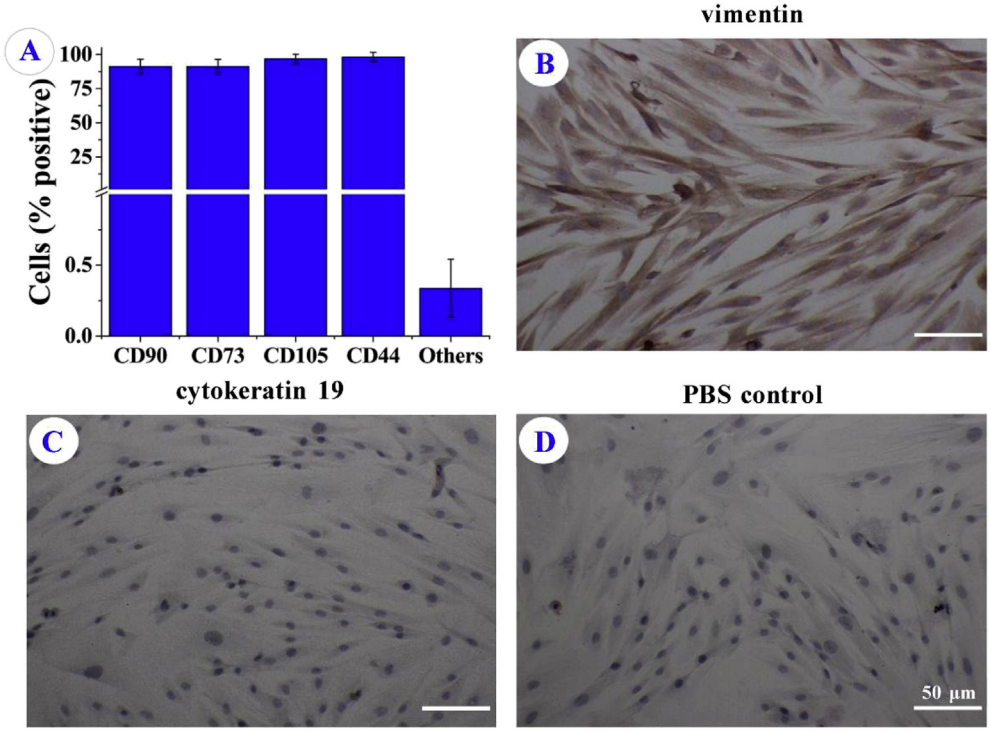

Fig. 1. Phenotype of hAMSCs. (A) Expression of cell surface antigens as determined by FCM analysis. The 'others' category includes CD45, CD34, CD11b, CD19, and HLA-DR; B-D: Protein expression analysis by immunohistochemical staining (scale bar: 50 μm; 100× magnification); (B) vimentin; (C) cytokeratin 19; (D) PBS control.

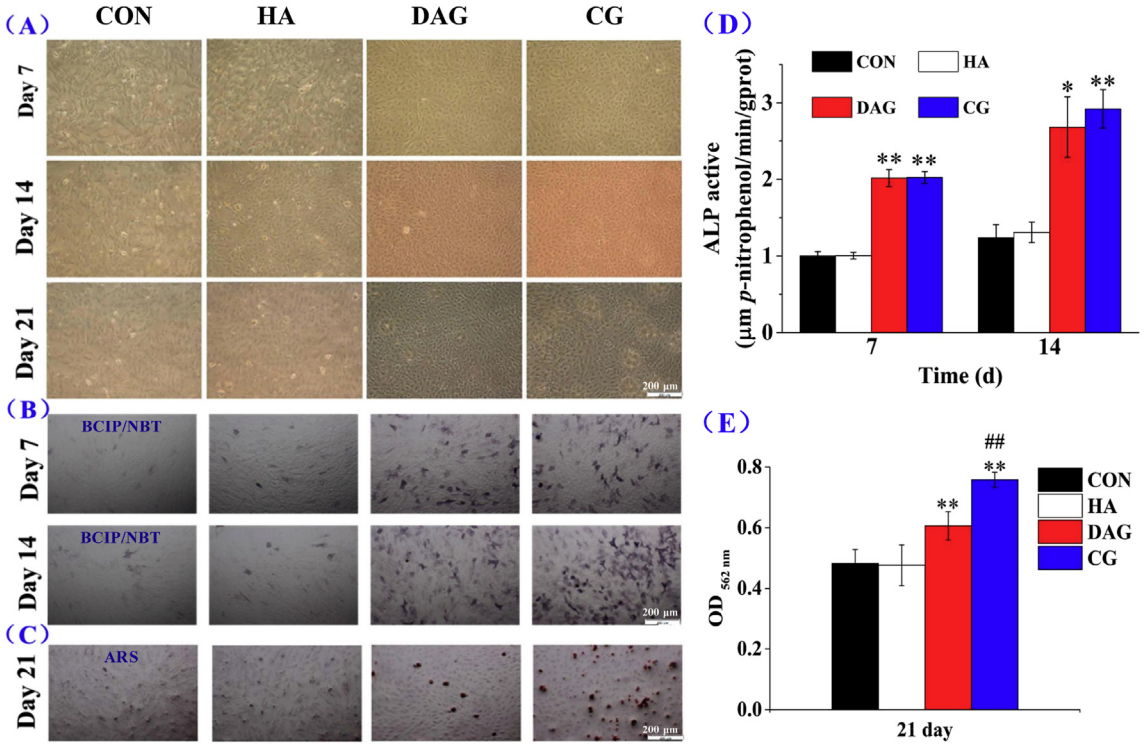

Fig. 2. Effect of HA on hAMSCs osteogenic differentiation. (A) Morphological changes of hAMSCs on days 7, 14, and 21 (scale bar: 200 μm; 40× magnification); (B) ALP expression as assessed by BCIP/NBT staining on days 7 and 14 (scale bar: 200 μm; 40× magnification); (C) Cell mineralization, as determined by Alizarin red S staining, on day 21 (scale bar: 200 μm; 40× magnification); (D) ALP activity, as determined by a colorimetric method; (E) ARS quantification, as determined by a colorimetric method. CON: negative control group; HA: HA treatment group; DAG: positive drug control group; CG: HG + DAG group. The data are expressed as the mean ± SD ($n = 3$). Compared with CON, $^{*}P < 0.05$, $^{**}P < 0.01$; compared with DAG, $^{\#}P < 0.05$, $^{\#\#}P < 0.01$. (For interpretation of the references to colour in this figure legend, the reader is referred to the web version of this article.)

Ocn, *ALP*, and *Col1α1* at different stages during hAMSC osteogenic differentiation. As shown in Fig. 3, the expression levels of all of the genes tested were significantly higher in the CG group than in the CON and DAG groups on day 7. The expression levels of all of the genes tested then decreased on days 14 and 21 in the DAG and CG groups. Furthermore, most of the genes tested were expressed at higher levels in the CG group than in the DAG group on days 14 and 21, except for *Col1α1*. In addition, treatment with HA resulted in slightly increased

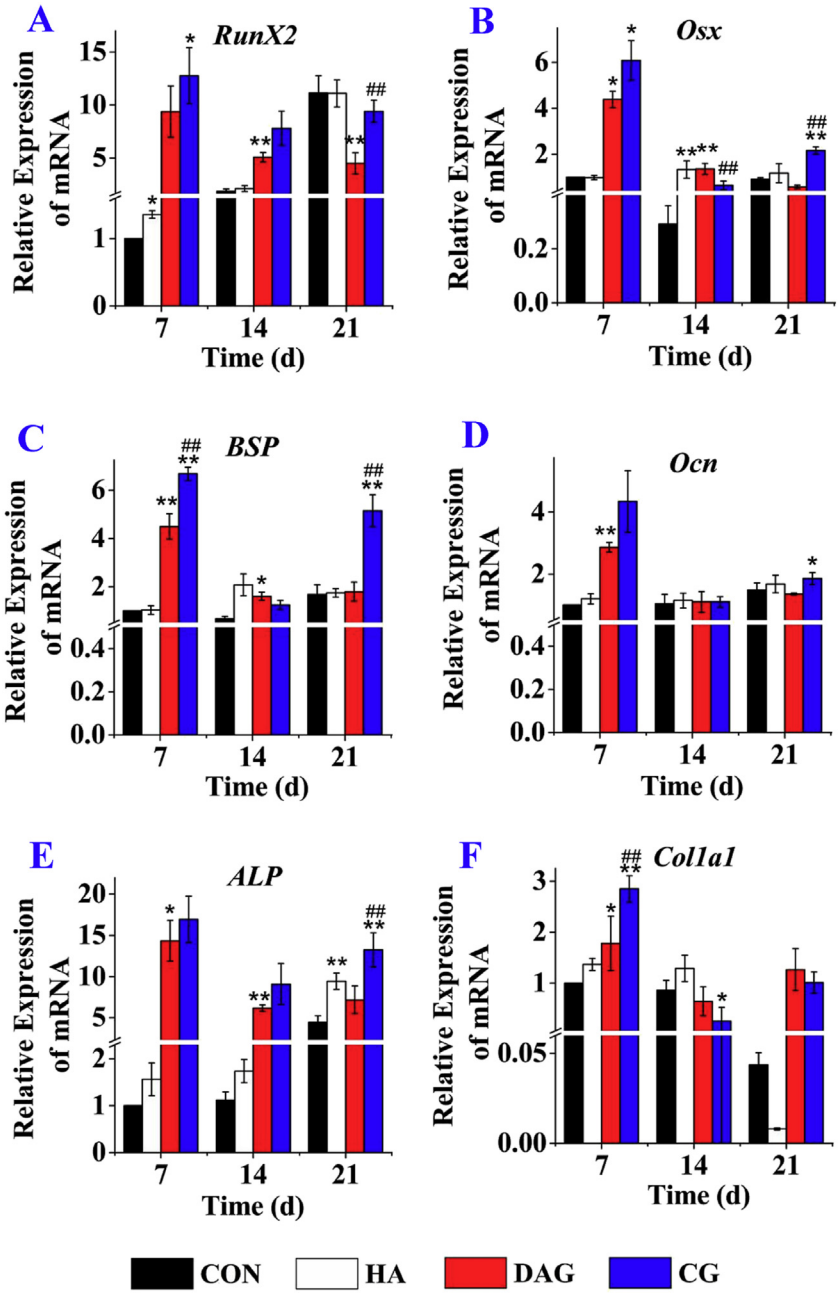

Fig. 3. Relative expression levels of osteogenesis-related genes in hAMSCs. (A) Relative expression level of *RunX2* mRNA; (B) Relative expression level of *Osx* mRNA; (C) Relative expression level of *BSP* mRNA; (D) Relative expression level of *Ocn* mRNA; (E) Relative expression level of *ALP* mRNA; (F) Relative expression level of *Col1α1* mRNA. CON: negative control group; HA: HA treatment group; DAG: positive drug control group; CG: HG + DAG. The data are expressed as the mean ± SD ($n = 3$). Compared with CON, $^{*}P < 0.05$, $^{**}P < 0.01$; compared with DAG, $^{\#}P < 0.05$, $^{\#\#}P < 0.01$.

expression levels of all of the genes tested at the different time points in comparison to CON, except for *Col1α1* on day 21. The expression of each gene tested remained at approximately the same level at each time point for the CON and HA treatment groups, with the exception of *Runx2* and *ALP*, which were markedly up-regulated, and *Col1α1*, which was remarkably down-regulated, on day 21. However, the expression levels of all of the osteogenic genes tested in the induction groups (DAG and CG) clearly decreased over the course of the hAMSC differentiation process. In addition, the trend in *Runx2* and *ALP* expression levels was consistent with the osteogenic differentiation period. Next, the expression levels of osteogenesis-associated proteins, including RunX2, Osx, BSP, ALP, and Col1α1, were determined, as shown in Figs. 4A and B. The changes in protein expression were not completely synchronized with the changes in transcription over the course of the osteogenic differentiation process, especially for RunX2, BSP, and Col1α1. For example, Runx2 expression was essentially consistent for all of the treatment groups on days 7 and 14, except for the DAG group on day 14. Runx2 expression increased by about 1.5-fold for the HA group and 2-fold for the DAG and CG groups by day 21 (Fig. 4B-a). Similarly, inconsistent with the mRNA findings were the protein levels of BSP and Col1α1, which increased from day 7 and peaked at day 14 in the DAG and CG groups. Furthermore, BSP and Col1α1 were expressed at slightly lower levels in the CG group than in the DAG group at these time points (Figs. 4B-c and -e). However, treatment with HA alone resulted in the increased expression of Runx2, Osx, BSP, and ALP compared with the negative control group at day 21, and Runx2, BSP, and ALP expression were higher in the CG group than in the DAG group. However, in contrast to the ALP gene expression results (Fig. 3), the

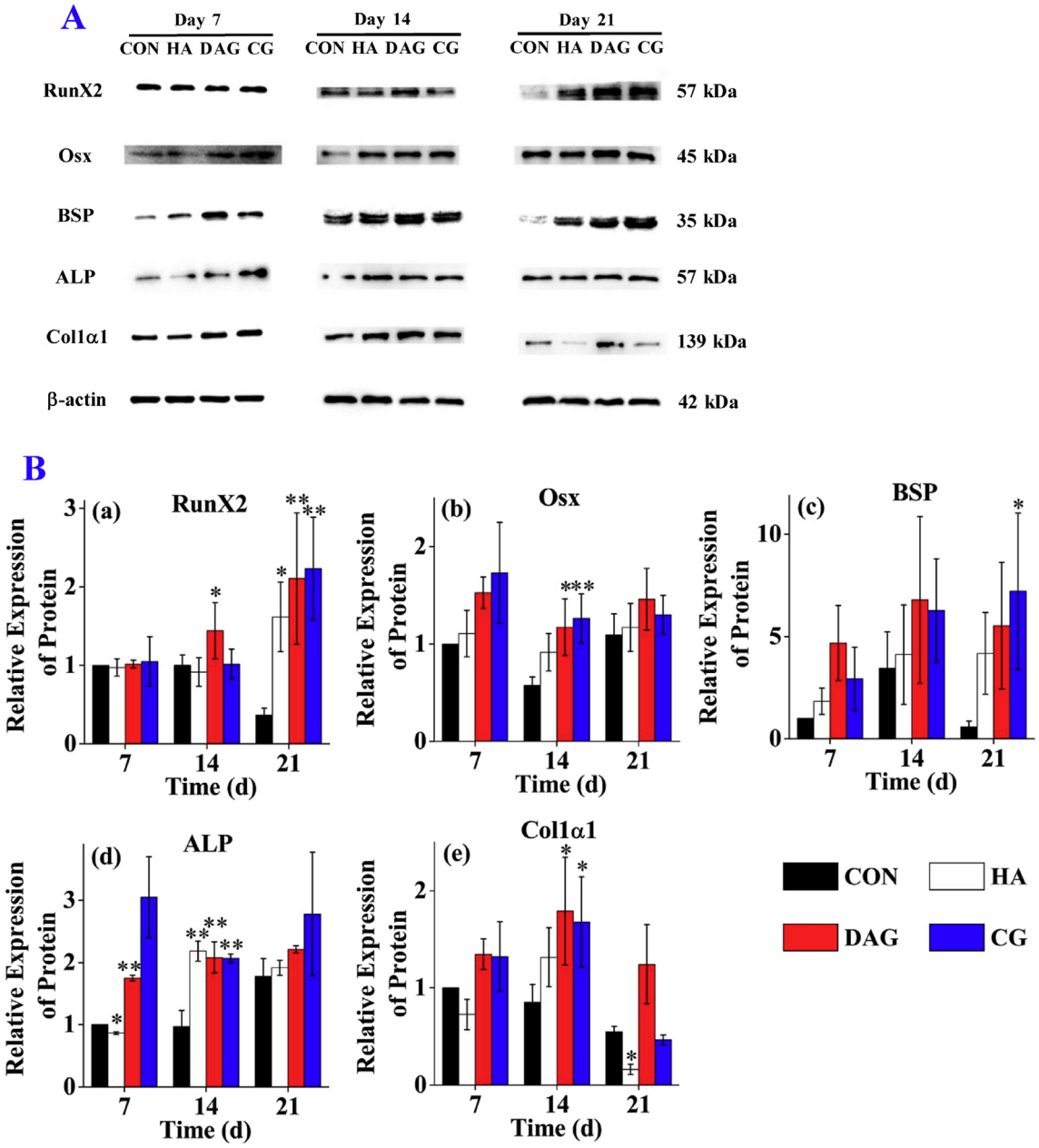

Fig. 4. Relative expression levels of osteogenesis-related proteins in hAMSCs. (A) Western blotting results; (B) Quantification of the blots; (a) Relative expression level of RunX2; (b): Relative expression level of Osx; (c): Relative expression level of BSP; (d): Relative expression level of ALP; (e): Relative expression level of Col1α1. CON: negative control group; HA: HA treatment group; DAG: positive drug control group; CG: HG + DAG. The data are expressed as the mean ± SD (n = 3). Compared with CON, $*P < 0.05$, $**P < 0.01$.

synergistic effect of HA and DAG on osteoinduction was not evident from the ALP protein assay results (Fig. 4).

3.4. Effect of HA on stemness-related genes in hAMSCs during osteogenic differentiation

To investigate the changes in stemness-related gene expression during the osteogenic differentiation of hAMSCs, the expression of *Oct4* and *Nanog* was examined on days 7, 14, and 21. As shown in Fig. 5, the stemness genes tested were expressed at relatively stable levels in the CON group throughout the entire time course. At early time points, the expression levels of these stemness genes were significantly higher in the DAG and CG groups than in the other groups. Similar results were observed on day 21. Interestingly, treatment with HA alone resulted in increased expression of the stemness genes tested. Furthermore, combined treatment with HA and DAG (CG group) had a positive synergistic effect on the expression of stemness genes at days 7 and 21.

3.5. 3.5 HA promotes osteogenic differentiation by activating the TGF-β/Smad signalling pathway

A human osteogenesis RT^2 Profiler PCR array was used to measure the expression of 84 genes involved in signalling pathways, as shown in Table 2, and to determine the involvement of specific signalling pathways in the observed effect of HA on hAMSC osteogenic differentiation. The candidate genes were selected on the basis of the absolute value (not < 2) of fold change of gene expression levels. The results from the RT^2 Profiler PCR array showed that 19 genes that are typically activated during osteogenic differentiation were significantly up-regulated or down-regulated by at least 2-fold in the hAMSCs treated with

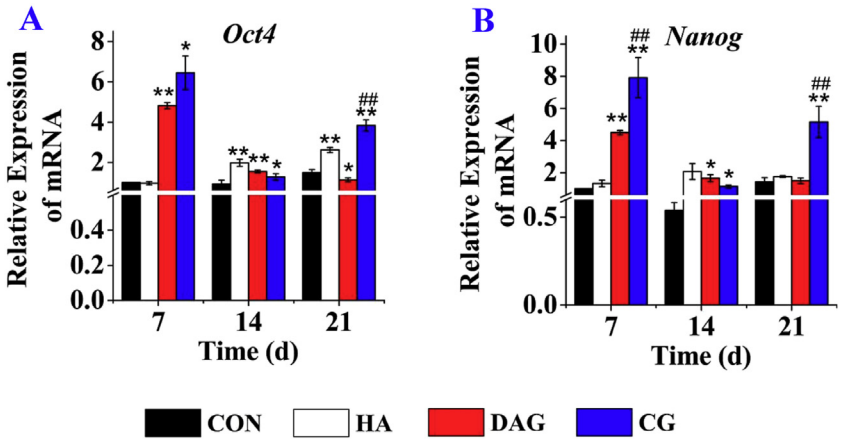

Fig. 5. Relative expression levels of stemness-related genes in hAMSCs. (A) Relative expression level of *Oct4*; (B) Relative expression level of *Nanog*. CON: negative control group; HA: HA treatment group; DAG: positive drug control group; CG: HG + DAG. The data are expressed as mean ± SD (n = 3). Compared with CON, $^{*}P < 0.05$, $^{**}P < 0.01$; compared with DAG, $^{\#}P < 0.05$, $^{\#\#}P < 0.01$.

HA + DAG group as compared with the DAG group (Fig. 6), and that their expression levels were associated with different stages of hAMSC osteogenic differentiation. For example, *ACVR1*, *BMP3*, *BMP5*, *BMPR1β*, *CHRD*, *FGF1*, *SMAD2*, *SPP1*, and *TNF* were significantly up-regulated on day 7 and then down-regulated on day 14. Based on the different genes identified by this screening process, we concluded that the TGF-β/Smad signalling pathway was involved in mediating the synergistic promotion of osteogenic differentiation of hAMSCs by HA and DAG. Next, SB431542 (10 mM), a potent and selective inhibitor of TGF-β signalling, was used to treat cells in the DAG and CG treatment group during osteogenic differentiation of hAMSCs. As shown in Fig. 7A, the CG group exhibited greater ALP staining than the DAG group after 7 days of treatment, as mentioned above. The addition of SB431542 resulted in a notable decrease in ALP staining in the CG group but had no effect on ALP staining in the DAG group. Treatment with SB431542 also inhibited the pro-differentiation effect of CG, which resulted in a notable down-regulation of the expression of the osteogenesis-associated genes *RunX2*, *Osx*, and *Ocn*, and especially *ALP* and *Col1α1*, in the CG group (Fig. 7B). The addition of SB431542 to the DAG group only had a slight, if any, effect on the expression of these genes. Finally, we determined the expression levels of some of the key transcription factors involving the TGF-β/Smad signalling pathway, including *TGF-β2*, *BMP5*, and *GDF10*, and *Smad2*, *3*, *4*, and *5*, in the DAG and CG groups. As shown in Fig. 7C, treatment with CG resulted in a significant increase in the expression of most of these factors compared to DAG treatment. Furthermore, the addition of SB431542 markedly inhibited the expression of these factors in the CG group, and only had a slight, if any, effect on the expression of these factors in the DAG group.

4. Discussion

hAMSCs are an important resource for tissue regeneration, repair, and reconstruction owing to their stemness properties and capacity for

Table 2
The 84 genes of interest representing human osteogenesis pathways tested in this study.

Skeletal Development						
ACVR1 (ALK2)	*BMPR1β (ALK6)*	*COL2A1*	*SOX9*	*BMP1*	*AHSG*	*BGLAP*
BMPR1α (ALK3)	*CSF1 (MCSF)*	*BMP5*	*BMP6*	*BMP7*	*BMP3*	*BMP4*
EGFR (ERBβ1)	*FGF2 (BFGF)*	*COL2α1*	*COL1α1*	*CTSK*	*DLX5*	*CHRD*
GDF10 (BMP3B)	*SMAD1 (MADH1)*	*IGF1*	*IGF1R*	*IGF2*	*IHH*	*MMP2*
SMAD3 (MADH3)	*TGFβR1 (ALK5)*	*NOG*	*RUNX2*	*SOX9*	*SP7*	*SPP1*
TNFSF11 (RANKL)	*TGFβ2*	*TWIST1*	*BGLAP*	*BMP2*	*TNF*	*TGFβ3*
ALPL	*COMP*	*FGFR1*	*CDH11*	*TGFβR2*	*MMP9*	*BMP1*
BMPR2	*GLI1*	*MMP8*	*TGFβ1*	*FGFR2*		
Bone Mineral Metabolism						
ACVR1 (ALK2)	*BMPR1α (ALK3)*	*BGLAP*	*BMP2*	*BMP4*	*BMP6*	*BMP7*
BMPR1β (ALK6)	*SMAD3 (MADH3)*	*IGF1*	*ANXA5*	*SOX9*	*TGFβ1*	*TGFβ3*
FGF2(BFGF)	*CDH11*	*COMP*	*EGF*	*GFB1*	*ITGβ1*	*MMP2*
VDR	*BMPR2*	*FGFR2*	*CALCR*	*AHSG*	*TWIST1*	*MMP8*
Extracellular Matrix Molecules						
FLT1(VEGFR1)	*COL14α1*	*COL15α1*	*COL1α1*	*COL1α2*	*COL2α1*	*COL3α1*
SERPINH1 (HSP47)	*COL10α1*	*MMP10*	*MMP2*	*MMP8*	*MMP9*	*PHEX*
AHSG	*CTSK*	*BGN*	*COL5α1*	*ALPL*		
Cell Adhesion Molecules						
EGFR (ERBβ1)	*BMPR1β (ALK6)*	*CDH11*	*COL14α1*	*COL2α1*	*BMP1*	*ICAM1*
TNFSF11(RANKL)	*CSF1(MCSF)*	*TNF*	*FN1*	*VCAM1*	*CD36*	*COL3α1*
SMAD3(MADH3)	*ITGα3*	*ITGαM*	*ITGβ1*	*IHH*	*BGLAP*	*COL15α1*
COMP	*SOX9*	*TGFβ1*	*ITGα2*	*ITGα1*	*COL5α1*	
Growth Factors						
CSF2 (GM-CSF)	*CSF3 (GCSF)*	*EGF*	*FGF1*	*IGF1*	*IGF2*	*PDGFA*
FGF2 (BFGF)	*GDF10 (BMP3B)*	*VEGFA*	*VEGFB*			
Transcription Factors						
SMAD1 (MADH1)	*SMAD2 (MADH2)*	*TWIST1*	*RUNX2*	*SOX9*	*GLI1*	*NFκB1*
SMAD3 (MADH3)	*SMAD4 (MADH4)*	*SMAD5 (MADH5)*				

A

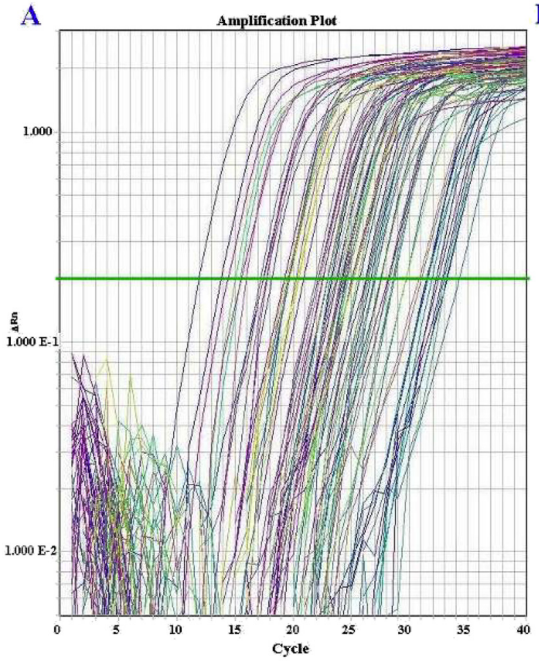

B

Gene	Fold-change			GenBank ID	Description
	Day7	Day14	Day21		
ACVR1	**2.11**	1.10	-1.04	NM_001105	activin A receptor, type I
AHSG	-1.11	1.60	**-3.58**	NM_001622	alpha-2-HS-glycoprotein
ALPL	1.09	**2.12**	-1.18	NM_000478	alkaline phosphatase, tissue-nonspecific isozyme
BMP3	**2.22**	-1.55	-1.29	NM_001201	bone morphogenetic protein 3
BMP5	**10.22**	1.44	**5.05**	NM_021073	bone morphogenetic protein 5
BMPR1β	**2.28**	**-2.30**	1.97	NM_001203	bone morphogenetic protein receptor, type I beta
CALCR	-1.33	-1.46	**3.65**	NM_001742	calcitonin receptor
CHRD	**2.30**	-1.08	1.02	NM_003741	chordin
COL2α1	1.48	1.18	**-2.31**	NM_001844	collagen, type II, alpha 1
CSF3	1.26	**-2.40**	1.44	NM_000759	colony stimulating factor 3 (granulocyte)
FGF1	**2.03**	1.53	-1.03	NM_000800	fibroblast growth factor 1 (acidic)
FGFR1	1.65	**-3.92**	1.03	NM_015850	fibroblast growth factor receptor 1
GDF10	1.34	**19.37**	**2.67**	NM_004962	growth differentiation factor 10
MMP10	-1.04	1.03	**-2.65**	NM_002425	matrix metallopeptidase 10 (stromelysin 2)
SMAD2	**2.48**	-1.27	-1.04	NM_005901	SMAD family member 2
SPP1	**2.01**	1.42	1.07	NM_000582	secreted phosphoprotein 1
TNF	**4.52**	-1.03	**-3.26**	NM_000594	tumor necrosis factor
TNFSF11	-1.34	**3.22**	-1.53	NM_003701	tumor necrosis factor (ligand) superfamily, member 11
VCAM1	1.00	**2.70**	-1.40	NM_001078	vascular cell adhesion molecule 1
β2M	**2.16**	1.37	1.03	NM_004048	beta-2-microglobulin

Note: CG vs PG

Fig. 6. Differential osteogenic differentiation gene expression profiles induced by treatment with CG and DAG in hAMSCs, as determined by PCR array. (A) Representative PCR array amplification curve of one sample after CG treatment; (B) Genes whose expression changed > 2-fold between samples, as indicated by the PCR array.

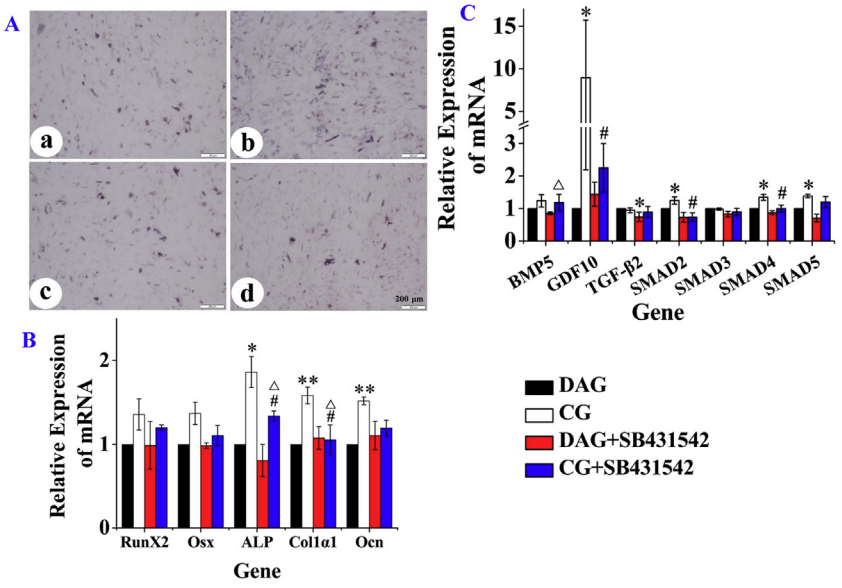

Fig. 7. Synergistic mechanism analysis of HA-induced osteogenic differentiation in hAMSCs. (A) Expression of ALP, as determined by staining, on day 7 (a: DAG; b: CG; c: DAG + SB431542; d: CG + SB431542; scale bar: 200 μm; 40× magnification); (B) Relative expression levels of osteogenesis-related genes on day 7; (C) Relative expression levels of TGF-β signalling pathway associated-genes on day 7; DAG: positive drug control group; CG: HG + DAG; The data are expressed as the mean ± SD (n = 3). The final concentration of SB431542 was 10 mM. Compared with DAG $^{*}P < 0.05$, $^{**}P < 0.01$; compared with CG $^{\#}P < 0.05$, $^{\#\#}P < 0.01$; compared with DAG + SB431542 group $^{\triangle}P < 0.05$, $^{\triangle\triangle}P < 0.01$.

multilineage differentiation. In this study, we investigated the ability of HA to induce osteogenesis in hAMSCs and the underlying mechanism of this process. Our data showed that HA alone was able to enhance the expression of some osteoblast-specific genes in hAMSCs but did not induce ALP activity or promote the formation of mineralized nodules. However, HA worked synergistically with DAG (a standard cocktail for inducing the osteogenic differentiation of stem cells) to promote hAMSC differentiation into osteoblasts, potentially *via* the TGF-β/BMP signalling pathway.

HA is a polysaccharide and the activity of polysaccharides is closely related to their MWs. The regulation of osteoblast differentiation by HA similarly depends on its MW. As described previously, low MW HA (60 kDa) inhibits osteoblastic differentiation, and high MW HA (900 kDa, 2300 kDa) facilitates osteoblastic differentiation in rat calvarial-derived cells [9]. High MW HA (2000 kDa) potentiates BMP-2-induced osteoblastic differentiation in human osteoblastic lineage MG63 cells *via* the down-regulation of antagonists and ERK phosphorylation [11]. Recent data have also shown that high MW HA (1110–2630 kDa) increases the expression of typical osteogenic differentiation genes, such as *ALP*, *Runx-2*, and *Ocn,* at the mRNA level in rabbit bone marrow-derived stem cells. Furthermore, *ALP*, *Runx-2,* and *Ocn* mRNAs are expressed in a MW-dependent manner. The higher the MW of HA, the higher the mRNA expression [17]. In contrast, other research groups have shown that the osteoblastic differentiation induced by BMP-2 in C2C12 cells (mouse myoblastic cells) and ST2 cells (mouse bone marrow cells) is significantly down-regulated by high MW

HA (900–1200 kDa), and high MW HA negatively regulates osteoblastic differentiation *via* the CD44 receptor when over 80% of the C2C12 and ST2 cells are CD44-positive [10]. High MW HA (2000 kDa) does not promote the expression of osteogenesis-related genes, including *ALP*, *Ocn*, *Opn*, and *BMP-2*, at the mRNA level in human periodontal ligament cells [18]. Therefore, the effect of HA on osteogenic differentiation is debatable. In this study, we show for the first time that low MW HA (300 kDa) can regulate osteogenic differentiation in hAMSCs. Positive osteogenesis inducer enhanced osteogenic differentiation of hAMSCs but this effect was shown to be enhanced by addition of HA. These findings are in agreement with previous studies that found that high MW HA inhibits cell differentiation [10,18], but contradict other studies [9,17]. Therefore, we concluded that HA-mediated regulation of osteoblast differentiation may be cell type-dependent. HA participates in many cellular functions *via* receptors, such CD44, RHAMM, and TLR4; CD44 is the main HA receptor, and RHAMM can compensate for the loss of CD44 [10,17]. However, there are significant differences in the expression levels and types of HA receptors in different cell types. For example, CD44 is highly expressed by mesenchymal stem cells (including hAMSCs) but is absent or only expressed at low levels in human amniotic epithelial cells. Thus, it is possible that HA interacts with different receptors to affect various cell events in different cell types, such that its effects are not only dependent on MW.

The osteogenic differentiation of MSCs *in vitro* is usually divided into three stages: the cell proliferation stage, early cell differentiation stage, and later cell differentiation stage [19]. Cell proliferation is significantly enhanced when human MSCs are cultivated for longer periods with the routinely used osteogenic inducer DAG. After the initial adhesion and proliferation of human MSCs, their maturation into the osteogenic lineage is an essential step for osteogenesis [20]. The cell maturation and mineralization that takes place during osteogenesis is tightly regulated by signalling molecules, including hormones, cytokines, and transcription factors. Runx2 is a master osteogenic transcription factor [21], particularly at the early stage of osteoblast differentiation. Runx2 induces osteoblast differentiation by promoting the transcription and translation of key osteogenic genes, such as *Col1α1*, *Ocn*, *BSP*, and *Opn*, by binding to the osteoblast-specific element at the early stage of differentiation, and induces calcification by increasing ALP activity [22,23]. Previous studies have demonstrated that the major component in DAG, DXM, promotes mesenchymal stem cell proliferation [24] and induces mesenchymal stem cell differentiation into osteoblasts by activating Runx2 expression through a FHL2/β-catenin signalling-dependent mechanism in which DXM induces the up-regulation of the endogenous activator FHL2, the interaction of FHL2 and β-catenin in the presence of Wnt3a potentiates β-catenin nuclear translocation, and the binding of nuclear β-catenin to TCF/LEF leads to Runx2 transcription [25]. We previously showed that HA increases the expression of Wnt3a, cyclin D1, and β-catenin in hAMSCs and promotes hAMSC proliferation by activating canonical Wnt/β-catenin signalling [4]. In the present study, we found that HA acted synergistically with the osteogenesis inducer DAG, leading to higher transcription levels of all of the osteogenesis-related genes tested, including *Runx2*, *Ocn*, *Col1α1*, *ALP*, *Osx*, and *BSP* in hAMSCs, in comparison to the negative control group and/or the positive control group (which was treated with DAG only). Furthermore, in the early stage of differentiation, HA alone significantly promoted Runx2 expression in hAMSCs 7 days post-treatment. These findings suggest that HA behaves similarly to DXM by signalling *via* Wnt at the early stage of osteoinduction differentiation in mesenchymal stem cells. In addition, our results showed that HA significantly increased ALP activity on day 14 and mineralization on day 21 in hAMSCs in the late stage of differentiation, and acted synergistically with DAG to induce osteogenesis osteoinduction, as determined by ALP activity and the degree of calcium deposition. Therefore, HA in combination with DAG may enhance osteogenic differentiation in hAMSCs by up-regulating the expression of the key osteogenesis-related gene *RUNX2* at the early differentiation stage.

In this study, a distinct non-synchronous change between mRNA and protein expression levels was observed for most of the osteoblast-specific factors tested during hAMSC osteoinduction differentiation. For example, ALP mRNA expression induced by DAG peaked at day 7, decreased sharply at day 14, then remained constant over time (Fig. 3E), whereas the ALP protein level increased progressively over time (Fig. 4B-d). This is consistent with a previous study [26]. However, treatment with HA and DAG resulted in a bimodal pattern of ALP mRNA expression, *i.e.*, ALP mRNA expression peaked at day 7, decreased at day 14, and peaked again at day 21 (Fig. 3E). Furthermore, ALP protein expression (Fig. 4B-d) in the CG group was consistent with its mRNA expression (Fig. 3E) over the course of the hAMSC osteogenic differentiation process. This suggests that CG and DAG may induce osteogenic differentiation by distinct mechanisms.

The biochemical signals by which HA induces an osteogenic response in stem cells are yet to be fully elucidated. In humans, there are at least 15 bone morphogenic proteins (BMPs), which belong to the TGF-β superfamily. BMPs, especially BMP-2, 6, and 9, are known to promote osteogenesis, strongly induce the osteoblast differentiation of mesenchymal stem cells *in vitro*, and are the most osteogenic BMPs *in vivo* [10,11,27]. Furthermore, signal transduction studies have shown that Smad1, 5, and 8 are the immediate downstream molecules of the above-mentioned BMP receptors and play a central role in osteogenic differentiation [10,28]. Thus, the Smad-dependent BMP signalling pathway plays an important role in the osteogenic differentiation of mesenchymal stem cells. Accordingly, we hypothesized that the synergistic osteogenic effect induced by HA and DAG in hAMSCs was regulated by the Smad-dependent BMP signalling pathway. A human osteogenesis RT^2 Profiler PCR Array was employed at three different time points in the study. The results showed that most of the genes whose expression levels were affected by combined treatment with HA and DAG were involved in the TGF-β/BMP signalling pathway at the early differentiation stage. Furthermore, ALP, Col1α1, and Ocn mRNA expression was significantly reduced in the CG group (which was treated with both HA and DAG) when the TGF-β/BMP signalling pathway was blocked, while the expression of Runx2 and Osx did not change. In addition, there was no change in the expression levels of any of the tested genes in the DAG group when this signalling pathway was blocked. As mentioned above, the osteogenic differentiation of stem cells is a multistep and complex physiological process, and it is very inefficient to stimulate differentiation by a single factor or method. Just as bone tissue engineering focuses on three key elements, *i.e.* seed cells, biological growth factors, and biocompatible scaffolds, to enhance bone formation and repair *in vivo*, the synergistic effect of multiple factors can be applied as an attractive strategy for the osteogenic differentiation of stem cells *in vitro*. For example, shin et al. found that the combination of proper mechanical stretching and epigallocatechin-3-gallate (EGCG) promoted the osteogenic differentiation of human mesenchymal stem cells (hMSCs) [29]. Carvalho et al. also demonstrated that the supplement of osteopontin (OPN) and osteocalcin (OC) in the osteogenic differentiation medium enhanced osteogenic differentiation of human bone marrow mesenchymal stem/stromal cells (hBM MSC) [30]. Recently, similar to our work, cerium (one of the lanthanides), in combination with DAG, was shown to have a potent osteogenic differentiation-promoting effect on mouse bone marrow-derived mesenchymal stem cells, involved in activating the TGF-β/BMP signalling pathway [16]. Indeed, different signalling pathways with diverse functions may be involved in the osteogenic differentiation of mesenchymal stem cells. For example, BMP9, a potent osteogenic factor (as mentioned above), induces osteogenic differentiation in mesenchymal stem cells by initiating a well-coordinated cascade of diverse signalling events, including TGF-β/BMP, Wnt/β-catenin, Notch, and MAPKs [31]. Therefore, the mechanism by which HA combines with DAG to synergistically induce osteogenic differentiation in hAMSCs requires further elucidation.

In addition, combined treatment with HA and DAG significantly

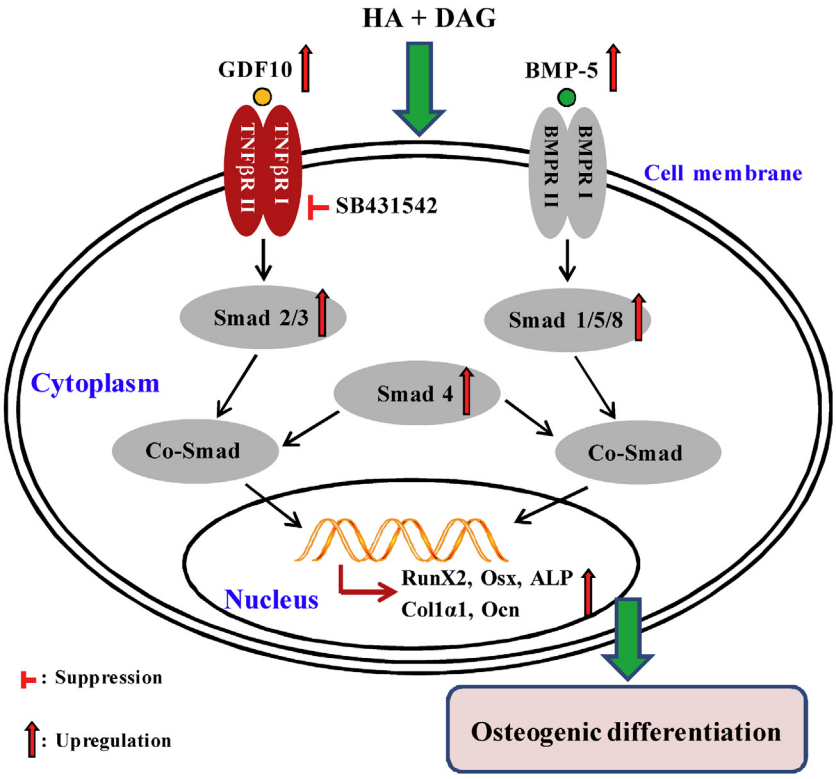

Fig. 8. A schematic diagram showing the proposed mechanism of HA in combination with DAG enhanced the osteogenic differentiation of hAMSCs through the TGF-β/Smad signalling pathway.

promoted the transcription of the stemness genes *Oct4* and *Nanog* at the early and/or late differentiation stages of hAMSC osteogenic differentiation. Oct4 and Nanog are essential transcription factors that regulate the stemness properties (self-renewal and pluripotency) of stem cells. As described previously [32–34], Oct4 and Nanog control a cascade of signalling pathways that are intricately connected to the regulation of self-renewal, differentiation, genome surveillance, and cell fate determination in stem cells. Furthermore, the up-regulation of Oct4 and Nanog maintains stemness and regenerative potential and inhibits the expression of aging-related genes and the aging of adult stem cells [35,36]. Therefore, harnessing the synergistic osteoinductive effects of HA and DAG could help promote bone repair in the context of regenerative medicine.

5. Conclusions

In conclusion, the present study demonstrated that treatment with HA alone, and especially in combination with DAG, up-regulates the expression of osteoblast-specific genes and promotes the osteogenic differentiation of hAMSCs through the TGF-β/BMP signalling pathway (Fig. 8). Harnessing the synergistic effect of HA and DAG could be used to enhance osteogenesis in the context of regenerative medicine.

Ethics approval and consent to participate

The study and use of the human amnion were approved by the Ethics Committee of Affiliated Hospital of Zunyi Medical University (Zunyi, China).

Consent for publication

Not applicable.

Funding

The authors are grateful to financial support from the Science and Technology Innovation Leading Academics of National High-level Personnel of Special Support Program (GKFZ-2018-29), National Natural Science Foundation of China (Nos. 81660363, 81260278; 81460156), Guizhou High-Level Innovative Talent Support Program (No. QKH-RC-20154028), and Science and Technology Foundation of Guizhou Province (No. QKH-2017-1422).

Authors' contributions

L-TZ participated in the performance of all experiments and wrote the manuscript. R-ML interpreted the experimental data and produced the tables and figures. YL participated in the cytochemical staining and immunohistochemical analysis. Y-JZ performed the flow cytometer analysis. D-XC participated in the study design. C-YY provided necessary advices and recommendations throughout the research. J-HX made substantial contributions to conception and design, and helped to draft the manuscript. All authors read and approved the final manuscript.

Availability of data and material

The data used to support the findings of this study are available from the corresponding author upon request.

Declaration of Competing Interest

The authors declare that there are no conflicts of interests regarding the publication of this paper.

Acknowledgement

We would like to thank the Center for Translational Medicine,

Affiliated Hospital of Zunyi Medical University for providing experimental sites.

References

[1] J. Messner, L. Johnson, D.M. Taylor, P. Harwood, S. Britten, P. Foster, Treatment and functional outcomes of complex tibial fractures in children and adolescents using the Ilizarov method, Bone Joint J 100-B (2018) 396–403.

[2] Y. Watanabe, N. Harada, K. Sato, S. Abe, K. Yamanaka, T. Matushita, Stem cell therapy: is there a future for reconstruction of large bone defects? Injury 47 (2016) 47–51.

[3] S. Díaz-Prado, E. Muiños-López, T. Hermida-Gómez, M.E. Rendal-Vázquez, I. Fuentes-Boquete, F.J. de Toro, F.J. Blanco, Isolation and characterization of mesenchymal stem cells from human amniotic membrane, Tissue Eng Part C Methods 17 (2011) 49–59.

[4] R.M. Liu, R.G. Sun, L.T. Zhang, Q.F. Zhang, D.X. Chen, J.J. Zhong, J.H. Xiao, Hyaluronic acid enhances proliferation of human amniotic mesenchymal stem cells through activation of Wnt/β-catenin signaling, Exp. Cell Res. 345 (2016) 218–229.

[5] J.M. Karp, G.S. Leng Teo, Mesenchymal stem cell homing: the devil is in the details, Cell Stem Cell 4 (2009) 206–216.

[6] J.Y. Lee, A.P. Spicer, Hyaluronan: a multifunctional, megaDalton, stealth molecule, Curr. Opin. Cell Biol. 12 (2000) 581–586.

[7] E.R. Bastow, S. Byers, S.B. Golub, C.E. Clarkin, A.A. Pitsillides, A.J. Fosang, Hyaluronan synthesis and degradation in cartilage and bone, Cell. Mol. Life Sci. 65 (2008) 395–413.

[8] P. Spessotto, F.M. Rossi, M. Degan, R. Di Francia, R. Perris, A. Colombatti, V. Gattei, Hyaluronan-CD44 interaction hampers migration of osteoclast-like cells by down-regulating MMP-9, J. Cell Biol. 158 (2002) 1133–1144.

[9] L. Huang, Y.Y. Cheng, P.L. Koo, K.M. Lee, L. Qin, J.C. Cheng, S.M. Kumta, The effect of hyaluronan on osteoblast proliferation and differentiation in rat calvarial-derived cell cultures, J. Biomed. Mater. Res. A 66 (2003) 880–884.

[10] K. Kaneko, C. Higuchi, Y. Kunugiza, K. Yoshida, T. Sakai, H. Yoshikawa, K. Nakata, Hyaluronan inhibits BMP-induced osteoblast differentiation, FEBS Lett. 589 (2015) 447–454.

[11] M. Kawano, W. Ariyoshi, K. Iwanaga, T. Okinaga, M. Habu, I. Yoshioka, K. Tominaga, T. Nishihara, Mechanism involved in enhancement of osteoblast differentiation by hyaluronic acid, Biochem. Biophys. Res. Commun. 405 (2011) 575–580.

[12] M. Kisiel, M.M. Martino, M. Ventura, J.A. Hubbell, J. Hilborn, D.A. Ossipov, Improving the osteogenic potential of BMP-2 with hyaluronic acid hydrogel modified with integrin-specific fibronectin fragment, Biomaterials 34 (2013) 704–712.

[13] S. Mathews, R. Bhonde, P.K. Gupta, S. Totey, A novel tripolymer coating demonstrating the synergistic effect of chitosan, collagen type 1 and hyaluronic acid on osteogenic differentiation of human bone marrow derived mesenchymal stem cells, Biochem. Biophys. Res. Commun. 414 (2011) 270–276.

[14] C.M. Kolf, S. Lin, H. Jeannine, R.S. Tuan, Nascent osteoblast matrix inhibits osteogenesis of human mesenchymal stem cells in vitro, Stem Cell Res Ther 6 (2015) 258.

[15] M. Dominici, K. Le Blanc, I. Mueller, I. Slaper-Cortenbach, F. Marini, D. Krause, R. Deans, A. Keating, D.J. Prockop, E. Horwitz, Minimal criteria for defining multipotent mesenchymal stromal cells. The International Society for Cellular Therapy position statement, Cytotherapy 8 (2006) 315–317.

[16] D.D. Liu, J.C. Zhang, Q. Zhang, S.X. Wang, M.S. Yang, TGF-β/BMP signaling pathway is involved in cerium-promoted osteogenic differentiation of mesenchymal stem cells, J. Cell. Biochem. 114 (2013) 1105–1114.

[17] N. Zhao, X. Wang, L. Qin, Z. Guo, D. Li, Effect of molecular weight and concentration of hyaluronan on cell proliferation and osteogenic differentiation in vitro, Biochem. Biophys. Res. Commun. 465 (2015) 569–574.

[18] K. Takeda, N. Sakai, H. Shiba, T. Nagahara, T. Fujita, M. Kajiya, T. Iwata, S. Matsuda, K. Kawahara, H. Kawaguchi, H. Kurihara, Characteristics of high-molecular-weight hyaluronic acid as a brain-derived neurotrophic factor scaffold in periodontal tissue regeneration, Tissue Eng Part A 17 (2011) 955–967.

[19] E. Birmingham, G.L. Niebur, P.E. McHugh, G. Shaw, F.P. Barry, L.M. McNamara, Osteogenic differentiation of mesenchymal stem cells is regulated by osteocyte and osteoblast cells in a simplified bone niche, Eur Cell Mater 23 (2012) 13–27.

[20] R. Hess, A. Jaeschke, H. Neubert, V. Hintze, S. Moeller, M. Schnabelrauch, H.P. Wiesmann, D.A. Hart, D. Scharnweber, Synergistic effect of defined artificial extracellular matrices and pulsed electric fields on osteogenic differentiation of human MSCs, Biomaterials 33 (2012) 8975–8985.

[21] D.Y. Kim, E.J. Kim, W.G. Jang, Piperine induces osteoblast differentiation through AMPK-dependent Runx2 expression, Biochem. Biophys. Res. Commun. 495 (2018) 1497–1502.

[22] A. Javed, G.L. Barnes, B.O. Jasanya, J.L. Stein, L. Gerstenfeld, J.B. Lian, G.S. Stein, Runt homology domain transcription factors (Runx, Cbfa, and AML) mediate repression of the bone sialoprotein promoter: evidence for promoter context-dependent activity of Cbfa proteins, Mol. Cell. Biol. 21 (2001) 2891–2905.

[23] T. Komori, Runx2, a multifunctional transcription factor in skeletal development, J. Cell. Biochem. 87 (2002) 1–8.

[24] H. Wang, B. Pang, Y. Li, D. Zhu, T. Pang, Y. Liu, Dexamethasone has variable effects on mesenchymal stromal cells, Cytotherapy 14 (2012) 424–430.

[25] F. Langenbach, J. Handschel, Effects of dexamethasone, ascorbic acid and β-glycerophosphate on the osteogenic differentiation of stem cells in vitro, Stem Cell Res Ther 4 (2013) 117.

[26] Z. Huang, E.R. Nelson, R.L. Smith, S.B. Goodman, The sequential expression profiles of growth factors from osteroprogenitors to osteoblasts in vitro, Tissue Eng Part A 13 (2007) 2311–2320.

[27] H.H. Luu, W.X. Song, X. Luo, D. Manning, J. Luo, Z.L. Deng, K.A. Sharff, A.G. Montag, R.C. Haydon, T.C. He, Distinct roles of bone morphogenetic proteins in osteogenic differentiation of mesenchymal stem cells, J. Orthop. Res. 25 (2007) 665–677.

[28] D. Chen, M. Zhao, G.R. Mundy, Bone morphogenetic proteins, Growth Factors 22 (2004) 233–241.

[29] J.W. Shin, Y. Wu, Y.G. Kang, J.K. Kim, H.J. Choi, J.W. Shin, The effects of epigallocatechin-3-gallate and mechanical stimulation on osteogenic differentiation of human mesenchymal stem cells: individual or synergistic effects, Tissue Eng Regen Med 14 (3) (2017) 307–315.

[30] M.S. Carvalho, J.M. Cabral, C.L. da Silva, D. Vashishth, Synergistic effect of extracellularly supplemented osteopontin and osteocalcin on stem cell proliferation, osteogenic differentiation, and angiogenic properties, J. Cell. Biochem. (2018) 1–15.

[31] J.D. Lamplot, J. Qin, G. Nan, J. Wang, X. Liu, L. Yin, J. Tomal, R. Li, W. Shui, H. Zhang, S.H. Kim, W. Zhang, J. Zhang, Y. Kong, S. Denduluri, M.R. Rogers, A. Pratt, R.C. Haydon, H.H. Luu, J. Angeles, L.L. Shi, T.C. He, BMP9 signaling in stem cell differentiation and osteogenesis, Am J Stem Cells 2 (2013) 1–21.

[32] Y.H. Loh, Q. Wu, J.L. Chew, V.B. Vega, W. Zhang, X. Chen, G. Bourque, J. George, B. Leong, J. Liu, K.Y. Wong, K.W. Sung, C.W. Lee, X.D. Zhao, K.P. Chiu, L. Lipovich, V.A. Kuznetsov, P. Robson, L.W. Stanton, C.L. Wei, Y. Ruan, B. Lim, H.H. Ng, The Oct4 and Nanog transcription network regulates pluripotency in mouse embryonic stem cells, Nat. Genet. 38 (2006) 431–440.

[33] G. Pan, J.A. Thomson, Nanog and transcriptional networks in embryonic stem cell pluripotency, Cell Res. 17 (2007) 42–49.

[34] J. Sheik Mohamed, P.M. Gaughwin, B. Lim, P. Robson, L. Lipovich, Conserved long noncoding RNAs transcriptionally regulated by Oct4 and Nanog modulate pluripotency in mouse embryonic stem cells, RNA 16 (2010) 324–337.

[35] Z.H. Xie, Y.J. Wu, The expression levels of the stem genes and aging-related genes are associated with mutual antagonism, Prog Biochem Biophy 41 (2014) 627–631.

[36] B. Das, R. Bayat-Mokhtari, M. Tsui, S. Lotfi, R. Tsuchida, D.W. Felsher, H. Yeger, HIF-2α suppresses p53 to enhance the stemness and regenerative potential of human embryonic stem cells, Stem Cells 30 (2012) 1685–1695.